Clemson University
College of Engineering and Science
Control and Robotics (CRB) Technical Report

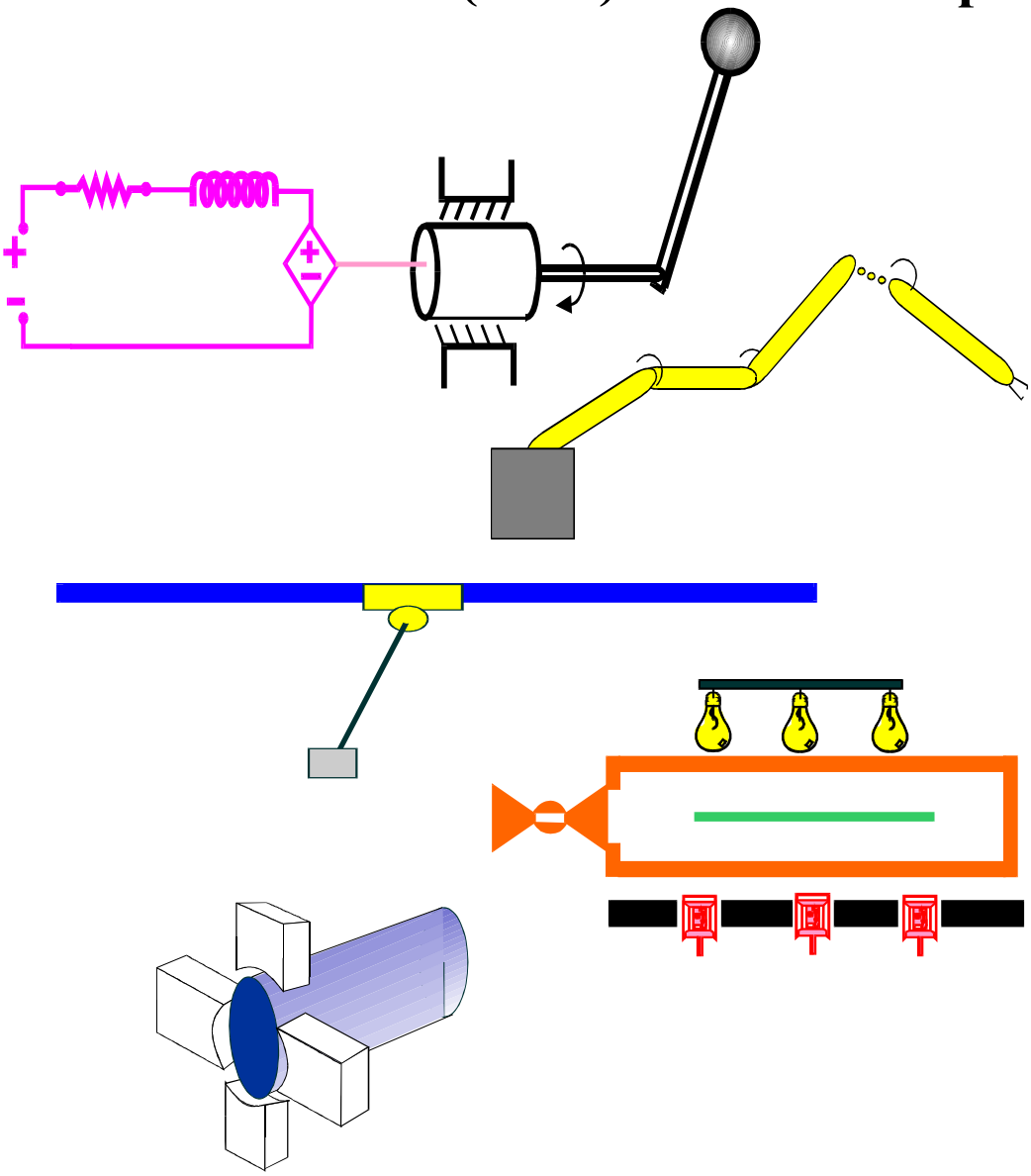

Number: CU/CRB/3/1/05/#1

Title: Navigation and Control of a Wheeled Mobile Robot

Authors: J. Chen, W. E. Dixon, D. M. Dawson, and T. Galluzzo

Report Documentation Page

Form Approved
OMB No. 0704-0188

1. REPORT DATE	2. REPORT TYPE	3. DATES COVERED
2005		**00-00-2005 to 00-00-2005**

4. TITLE AND SUBTITLE	5a. CONTRACT NUMBER
Navigation and Control of a Wheeled Mobile Robot	5b. GRANT NUMBER
	5c. PROGRAM ELEMENT NUMBER
6. AUTHOR(S)	5d. PROJECT NUMBER
	5e. TASK NUMBER
	5f. WORK UNIT NUMBER
7. PERFORMING ORGANIZATION NAME(S) AND ADDRESS(ES) **Clemson University,Department of Electrical & Computer Engineering,Clemson,SC,29634-0915**	8. PERFORMING ORGANIZATION REPORT NUMBER
9. SPONSORING/MONITORING AGENCY NAME(S) AND ADDRESS(ES)	10. SPONSOR/MONITOR'S ACRONYM(S)
	11. SPONSOR/MONITOR'S REPORT NUMBER(S)

12. DISTRIBUTION/AVAILABILITY STATEMENT
Approved for public release; distribution unlimited

13. SUPPLEMENTARY NOTES
The original document contains color images.

14. ABSTRACT

15. SUBJECT TERMS

16. SECURITY CLASSIFICATION OF:			17. LIMITATION OF ABSTRACT	18. NUMBER OF PAGES	19a. NAME OF RESPONSIBLE PERSON
a. REPORT	b. ABSTRACT	c. THIS PAGE			
unclassified	**unclassified**	**unclassified**		**11**	

Navigation and Control of a Wheeled Mobile Robot[1]

J. Chen,[†] W. E. Dixon[‡], D. M. Dawson[†], and T. Galluzzo[‡]

[†]Department of Electrical & Computer Engineering, Clemson University, Clemson, SC 29634-0915

[‡]Department of Mechanical & Aerospace Engineering, University of Florida, Gainesville, FL 32611

email: jian.chen@ieee.org, wdixon@ufl.edu, ddawson@ces.clemson.edu, galluzzt@ufl.edu

Abstract: Several approaches for incorporating navigation function approach into different controllers are developed in this paper for task execution by a nonholonomic system (e.g., a wheeled mobile robot) in the presence of known obstacles. The first approach is a path planning-based control with planning a desired path based on a 3-dimensional position and orientation information. A navigation-like function yields a path from an initial configuration inside the free configuration space of the mobile robot to a goal configuration. A differentiable, oscillator-based controller is then used to enable the mobile robot to follow the path and stop at the goal position. A second approach is developed for a navigation function that is constructed using 2-dimensional position information. A differentiable controller is proposed based on this navigation function that yields asymptotic convergence. Simulation results are provided to illustrate the performance of the second approach.

1 Introduction

Numerous researchers have proposed algorithms to address the motion control problem associated with robotic task execution in an obstacle cluttered environment. A comprehensive summary of techniques that address the classic geometric problem of constructing a collision-free path and traditional path planning algorithms is provided in Section 9, "Literature Landmarks", of Chapter 1 of [19]. Since the pioneering work by Khatib in [13], it is clear that the construction and use of potential functions has continued to be one of the mainstream approaches to robotic task execution among known obstacles. In short, potential functions produce a repulsive potential field around the robot workspace boundary and obstacles and an attractive potential field at the goal configuration. A comprehensive overview of research directed at potential functions is provided in [19]. One of criticisms of the potential function approach is that local minima can occur that can cause the robot to "get stuck" without reaching the goal position. Several researchers have proposed approaches to address the local minima issue (e.g., see [2], [3], [5], [14], [25]). One approach to address the local minima issue was provided by Koditschek in [16] for holonomic systems (see also [17] and [22]) that is based on a special kind of potential function, coined a navigation function, that has a refined mathematical structure which guarantees a unique minimum exists.

By leveraging from previous results directed at classic (holonomic) systems, more recent research has focused on the development of potential function-based approaches for more challenging nonholonomic systems (e.g., wheeled mobile robots (WMRs)). For example, Laumond et al. [18] used a geometric path planner to generate a collision-free path that ignores the nonholonomic constraints of a WMR, then divided the geometric path into smaller paths that satisfy the nonholonomic constraints, and then applied an optimization routine to reduce the path length. In [10] and [11], Guldner et al. use discontinuous, sliding mode controllers to force the position of a WMR to track the negative gradient of a potential function and to force the orientation to align with the negative gradient. In [1], [15], and [21], continuous potential field-based controllers are developed to also ensure position tracking of the negative gradient of a potential function, and orientation tracking of the negative gradient. More recently, Ge and Cui present a new repulsive potential function approach in [9] to address the case when the goal is nonreachable with obstacles nearby (GNRON). In [23] and [24], Tanner et al. exploit the navigation function research of [22] along with a dipolar potential field concept to develop a navigation function-based controller for a nonholonomic mobile manipulator. Specifically, the results in [23] and [24] use a discontinuous controller to track the negative gradient of the navigation function, where a nonsmooth dipolar potential field causes the WMR to turn in place at the goal position to align with a desired orientation.

In this paper, two different methods are proposed to achieve a navigation objective for a nonholonomic system. In the first approach, a 3-dimensional (3D)

[1]This work is supported in part by two DOC Grants, an ARO Automotive Center Grant, a DOE Contract, a Honda Corporation Grant, U.S. NSF Grant DMI-9457967, ONR Grant N00014-99-1-0589, and a DARPA Contract at Clemson University, and in part by AFOSR contract number F49620-03-1-0381 at the University of Florida.

navigation-like function-based desired trajectory is generated that is proven to ultimately approach to the goal position and orientation that is a unique minimum over the WMR free configuration space. A continuous control structure is then utilized that enables the WMR to follow the path and stop at the goal position and orientation setpoint (i.e., the controller solves the unified tracking and regulation problem). The unique aspect of this approach is that the WMR reaches the goal position with a desired orientation and is not required to turn in place as in many of the previous results. As described in [4] and [20], factors such as the radial reduction phenomena, the ability to more effectively penalize the robot for leaving the desired contour, the ability to incorporate invariance to the task execution speed, and the improved ability to achieve task coordination and synchronization provide motivation to encapsulate the desired trajectory in terms of the current position and orientation. For the on-line 2D problem, a continuous controller is designed to navigate the WMR along the negative gradient of a navigation function to the goal position. As in many of the previous results, the orientation for the on-line 2D approach requires additional development (e.g., a separate regulation controller; a dipolar potential field approach [23], [24]; or a virtual obstacle [9]) to align the WMR with a desired orientation. Simulation results are provided to illustrate the performance of the second approach.

2 Kinematic Model

The class of nonholonomic systems considered in this paper can be modeled as a kinematic wheel

$$\dot{q} = S(q)v \tag{1}$$

where $q(t)$, $\dot{q}(t) \in \mathbb{R}^3$ are defined as

$$q \triangleq [x_c \quad y_c \quad \theta]^T \qquad \dot{q} = \left[\dot{x}_c \quad \dot{y}_c \quad \dot{\theta}\right]^T. \tag{2}$$

In (1), the matrix $S(q) \in \mathbb{R}^{3\times 2}$ is defined as follows

$$S(q) \triangleq \begin{bmatrix} \cos\theta & 0 \\ \sin\theta & 0 \\ 0 & 1 \end{bmatrix} \tag{3}$$

and the velocity vector $v(t) \in \mathbb{R}^2$ is defined as

$$v \triangleq [v_c \quad \omega_c]^T \tag{4}$$

with $v_c(t), \omega_c(t) \in \mathbb{R}$ denoting the linear and angular velocity of the system. In (2), $x_c(t)$, $y_c(t)$, and $\theta(t) \in \mathbb{R}$ denote the position and orientation, respectively, $\dot{x}_c(t)$, $\dot{y}_c(t)$ denote the Cartesian components of the linear velocity, and $\dot{\theta}(t) \in \mathbb{R}$ denotes the angular velocity.

3 Control Objective

The control objective in this paper is to navigate a nonholonomic system (e.g., a wheeled mobile robot) along a collision-free path to a constant, goal position and orientation, denoted by $q^* \triangleq [x_c^* \quad y_c^* \quad \theta^*]^T \in \mathbb{R}^3$, in an obstacle cluttered environment with known obstacles. Specifically, the objective is to control the nonholonomic system along a path from an initial position and orientation to $q^* \in \mathcal{D}$, where $\mathcal{D}$ denotes a free configuration space. The free configuration space $\mathcal{D}$ is a subset of the whole configuration space with all configurations removed that involve a collision with an obstacle. To quantify the path planning-based control objective, the difference between the actual Cartesian position and orientation and the desired position and orientation, denoted by $q_d(t) \triangleq [x_{cd}(t) \quad y_{cd}(t) \quad \theta_d(t)]^T$, is defined as $e(t) \triangleq \left[\begin{array}{ccc} \tilde{x}(t) & \tilde{y}(t) & \tilde{\theta}(t) \end{array}\right]^T \in \mathbb{R}^3$ as follows

$$\tilde{x} \triangleq x_c - x_{cd} \qquad \tilde{y} \triangleq y_c - y_{cd} \qquad \tilde{\theta} \triangleq \theta - \theta_d \tag{5}$$

where the desired trajectory is designed so that $q_d(t) \to q^*$.

Motived by the navigation function approach in [16], a navigation-like function is utilized to generate the desired path $q_d(t)$. Specifically, the navigation-like function used in this paper is defined as follows

Definition 1 *Let $\mathcal{D}$ be a compact connected analytic manifold with boundary, and let q^* be a goal point in the interior of $\mathcal{D}$. The navigation-like function $\varphi(q) : \mathcal{D} \to [0, 1]$, is a function satisfy the following properties:*

1. $\varphi(q(t))$ is first order and second order differentiable (i.e., $\frac{\partial}{\partial q}\varphi(q(t))$and $\frac{\partial}{\partial q}\left(\frac{\partial}{\partial q}\varphi(q(t))\right)$ exist on $\mathcal{D}$).
2. $\varphi(q(t))$ obtains its maximum value on the boundary of $\mathcal{D}$.
3. $\varphi(q(t))$ has unique global minimum at $q(t) = q^*$.
4. If $\left\|\frac{\partial}{\partial q}\varphi(q(t))\right\|^2 \leq \varepsilon_z$, then $\|q(t) - q^*\| \leq \varepsilon_r$ with $\varepsilon_z, \varepsilon_r \in \mathbb{R}$ being known positive constants.
5. If $\varphi(q(t))$ is ultimately bounded by ε, then $\|q(t) - q^*\|$ is ultimately bounded by ε_r with $\varepsilon \in \mathbb{R}$ being some known positive constant.

4 Online 3D Path Planner

4.1 Trajectory Planning

The 3D desired trajectory can be generated online as follows

$$\dot{q}_d = -\varphi(q) \bigtriangledown \varphi(q) + v_r \tag{6}$$

where $\varphi(q) \in \mathbb{R}$ denotes a navigation-like function defined in Definition 1, $\bigtriangledown\varphi(q) \in \mathbb{R}^3$ denotes the gradient vector of $\varphi(q)$, and $v_r(t) \in \mathbb{R}^3$ is an additional control term to be designed.

Assumption The navigation-like function defined in Definition 1 along with the desired trajectory generated by (6) ensures an auxiliary terms $N(\cdot) \in \mathbb{R}^3$, defined as

$$N \triangleq \varphi(q_d) \bigtriangledown \varphi(q_d) - \varphi(q) \bigtriangledown \varphi(q), \quad (7)$$

satisfy the following inequality

$$\|N\| \leqslant \rho(q_d, e)\|e\| \quad (8)$$

where the positive function $\rho(\cdot)$ is nondecreasing in $\|q_d\|$ and $\|e\|$. The inequality given by (8) will be used in the subsequent stability analysis.

4.2 Model Transformation

To achieve the control objective, a controller must be designed to track the desired trajectory developed in (6) and stop at the goal position q^*. To this end, the unified tracking and regulation controller presented in [7] can be used. To develop the controller in [7], the open-loop error system defined in (5) must be transformed into a suitable form. Specifically, the position and orientation tracking error signals defined in (5) are related to the auxiliary tracking error variables $w(t) \in \mathbb{R}$ and $z(t) \triangleq \begin{bmatrix} z_1(t) & z_2(t) \end{bmatrix}^T \in \mathbb{R}^2$ through the following global invertible transformation [8]

$$\begin{bmatrix} w \\ z_1 \\ z_2 \end{bmatrix} \triangleq \begin{bmatrix} -\tilde{\theta}\cos\theta + 2\sin\theta & -\tilde{\theta}\sin\theta - 2\cos\theta & 0 \\ 0 & 0 & 1 \\ \cos\theta & \sin\theta & 0 \end{bmatrix} \begin{bmatrix} \tilde{x} \\ \tilde{y} \\ \tilde{\theta} \end{bmatrix}. \quad (9)$$

After taking the time derivative of (9) and using (1)-(5) and (9), the tracking error dynamics can be expressed in terms of the auxiliary variables defined in (9) as follows [8]

$$\begin{aligned} \dot{w} &= u^T J^T z + f \\ \dot{z} &= u \end{aligned} \quad (10)$$

where $J \in \mathbb{R}^{2\times 2}$ denotes a skew-symmetric matrix defined as

$$J \triangleq \begin{bmatrix} 0 & -1 \\ 1 & 0 \end{bmatrix}, \quad (11)$$

and $f(\theta, z_2, \dot{q}_d) \in \mathbb{R}$ is defined as

$$f \triangleq 2\begin{bmatrix} -\sin\theta & \cos\theta & z_2 \end{bmatrix}\dot{q}_d. \quad (12)$$

The auxiliary control input $u(t) \triangleq \begin{bmatrix} u_1(t) & u_2(t) \end{bmatrix}^T \in \mathbb{R}^2$ introduced in (10) is defined in terms of $v(t), \theta(t), \tilde{x}(t), \tilde{y}(t)$, and $\dot{q}_d(t)$ as follows

$$\begin{aligned} u &= \begin{bmatrix} 0 & 1 \\ 1 & -\tilde{x}\sin\theta + \tilde{y}\cos\theta \end{bmatrix} v \\ &\quad - \begin{bmatrix} \dot{\theta}_d \\ \dot{x}_d\cos\theta + \dot{y}_d\sin\theta \end{bmatrix}. \end{aligned} \quad (13)$$

4.3 Control Development

To facilitate the control development, an auxiliary error signal, denoted by $\tilde{z}(t) \in \mathbb{R}^2$, is defined as the difference between the subsequently designed dynamic oscillator-like signal $z_d(t) \in \mathbb{R}^2$ and the transformed variable $z(t)$, defined in (9), as follows

$$\tilde{z} = z_d - z. \quad (14)$$

Based on the open-loop kinematic system given in (10) and the subsequent stability analysis, we design $u(t)$ as follows [7]

$$u = u_a - k_2 z \quad (15)$$

where $k_2 \in \mathbb{R}$ is a positive, constant control gain. The auxiliary control term $u_a(t) \in \mathbb{R}^2$ introduced in (15) is defined as

$$u_a = \left(\frac{k_1 w + f}{\delta_d^2}\right) J z_d + \Omega_1 z_d, \quad (16)$$

where the auxiliary signal $z_d(t)$ is defined by the following differential equation and initial condition

$$\begin{aligned} \dot{z}_d &= \frac{\dot{\delta}_d}{\delta_d} z_d + \left(\frac{k_1 w + f}{\delta_d^2} + w\Omega_1\right) J z_d \\ z_d^T(0) z_d(0) &= \delta_d^2(0). \end{aligned} \quad (17)$$

The auxiliary terms $\Omega_1(w, f, t) \in \mathbb{R}$ and $\delta_d(t) \in \mathbb{R}$ are defined as

$$\Omega_1 = k_2 + \frac{\dot{\delta}_d}{\delta_d} + w\left(\frac{k_1 w + f}{\delta_d^2}\right) \quad (18)$$

and

$$\delta_d = \alpha_0 \exp(-\alpha_1 t) + \varepsilon_1 \quad (19)$$

respectively, k_1, α_0, α_1, $\varepsilon_1 \in \mathbb{R}$ are positive, constant control gains, and $f(\theta, z_2, \dot{q}_d)$ was defined in (12). As described in [8], motivation for the structure of (17) and (19) is based on the fact that

$$\|z_d\|^2 = \delta_d^2. \quad (20)$$

Based on (9), $e(t)$ can be expressed in terms of $w(t)$, $\tilde{z}(t)$, and $z_d(t)$ as follows

$$e = R_1 \begin{bmatrix} w \\ \tilde{z}_1 \\ \tilde{z}_2 \end{bmatrix} + R_2 \begin{bmatrix} z_{d1} \\ z_{d2} \end{bmatrix} \quad (21)$$

where $R_1(\cdot) \in \mathbb{R}^{3\times 3}, R_2(\cdot) \in \mathbb{R}^{3\times 2}$ are defined as follows

$$R_1 \triangleq \begin{bmatrix} \frac{1}{2}\cos\theta & -\frac{1}{2}z_{d2}\sin\theta & -\frac{1}{2}(z_1\sin\theta + 2\cos\theta) \\ -\frac{1}{2}\cos\theta & \frac{1}{2}z_{d2}\cos\theta & \frac{1}{2}(z_1\cos\theta - 2\sin\theta) \\ 0 & -1 & 0 \end{bmatrix} \quad (22)$$

$$R_2 \triangleq \begin{bmatrix} \frac{1}{2}z_{d2}\sin\theta & \cos\theta \\ -\frac{1}{2}z_{d2}\cos\theta & \sin\theta \\ 1 & 0 \end{bmatrix}. \quad (23)$$

Motivated by the subsequent stability analysis, the additional control term $v_r(t)$ in (6) is designed as follows

$$v_r = -k_3\rho_1^2 \bigtriangledown \varphi(q_d) - k_4\rho_2^2 \bigtriangledown \varphi(q_d) \tag{24}$$

where $k_3, k_4 \in \mathbb{R}$ denotes positive, constant control gains, and the positive functions $\rho_1(z_{d1}, z_1, q_d, e)$, $\rho_2(z_{d1}, z_1, q_d, e) \in \mathbb{R}$ are defined as follows

$$\rho_1 \triangleq \rho(q_d, e)\|R_1\| \qquad \rho_2 \triangleq \rho(q_d, e)\|R_2\| \tag{25}$$

4.4 Closed-loop Error System

After substituting (15) into (10), the dynamics for $w(t)$ can be obtained as follows

$$\dot{w} = u_a^T J\tilde{z} - u_a^T J z_d + f \tag{26}$$

where (14) and the properties of J in (11) were utilized. After substituting (16) into (26) for only the second occurrence of $u_a(t)$, utilizing (20) and the properties of J in (11), the final expression for the closed-loop error system for $w(t)$ can be obtained as follows

$$\dot{w} = u_a^T J\tilde{z} - k_1 w. \tag{27}$$

To determine the closed-loop error system for $\tilde{z}(t)$, we take the time derivative of (14) and then substitute (10) and (17) into the resulting expression to obtain the following expression

$$\dot{\tilde{z}} = \frac{\dot{\delta}_d}{\delta_d} z_d + \left(\frac{k_1 w + f}{\delta_d^2} + w\Omega_1\right) J z_d - u. \tag{28}$$

After substituting (15) and (16) into (28), (28) can be rewritten as follows

$$\dot{\tilde{z}} = \frac{\dot{\delta}_d}{\delta_d} z_d + w\Omega_1 J z_d - \Omega_1 z_d + k_2 z. \tag{29}$$

After substituting (18) into (29) for only the second occurrence of $\Omega_1(t)$ and then canceling common terms, the following expression can be obtained

$$\dot{\tilde{z}} = -k_2\tilde{z} + wJ\left[\left(\frac{k_1 w + f}{\delta_d^2}\right) J z_d + \Omega_1 z_d\right]. \tag{30}$$

Since the bracketed term in (30) is equal to $u_a(t)$ defined in (16), the final expression for the closed-loop error system for $\tilde{z}(t)$ can be obtained as follows

$$\dot{\tilde{z}} = -k_2\tilde{z} + wJu_a. \tag{31}$$

Remark 1 *Based on the fact that $\delta_d(t)$ of (19) exponentially approaches an arbitrarily small constant, the potential singularities in (16), (17), and (18) are always avoided.*

4.5 Stability Analysis

Theorem 1 *Provided $q_d(0) \in \mathcal{D}$, the desired trajectory generated by (6) along with the additional control term $v_r(t)$ designed in (24) ensures that $q_d(t) \in \mathcal{D}$ and $\|q_d(t) - q^*\| \leqslant \varepsilon_r$. where ε_r is defined in Definition 1.*

Proof: Let $V(t) \in \mathbb{R}$ denote the following function

$$V = kV_1 + V_2 \tag{32}$$

where $k \in \mathbb{R}$ is a positive constant, $V_1(t) \in \mathbb{R}$ denotes the following function

$$V_1 = \frac{1}{2}w^2 + \frac{1}{2}\tilde{z}^T\tilde{z} \tag{33}$$

and $V_2(q_d) : \mathcal{D} \to \mathbb{R}$ denotes a function as follows

$$V_2(q_d) \triangleq \varphi(q_d). \tag{34}$$

After taking the time derivative of (33) and then substituting (27) and (31) into the resulting expression and cancelling common terms, the following expression can be obtained

$$\dot{V}_1 = -k_1 w^2 - k_2\tilde{z}^T\tilde{z}. \tag{35}$$

After taking the time derivative of (34) and utilizing (6), the following expression can be obtained

$$\begin{aligned}\dot{V}_2(q_d) &= (\bigtriangledown\varphi(q_d))^T \dot{q}_d \\ &= -\|\bigtriangledown\varphi(q_d)\|^2 \varphi(q_d) \\ &\quad + (\bigtriangledown\varphi(q_d))^T N + (\bigtriangledown\varphi(q_d))^T v_r\end{aligned} \tag{36}$$

where $N(\cdot)$ is defined in (7). Based on (8), $\dot{V}_2(t)$ can be upper bounded as follows

$$\begin{aligned}\dot{V}_2 \leqslant\ & -\|\bigtriangledown\varphi(q_d)\|^2 \varphi(q_d) \\ & +\rho(q_d, e)\|\bigtriangledown\varphi(q_d)\|\|e\| + (\bigtriangledown\varphi(q_d))^T v_r.\end{aligned} \tag{37}$$

After substituting (21) into (37), the following inequality can be obtained

$$\begin{aligned}\dot{V}_2 \leqslant\ & -\|\bigtriangledown\varphi(q_d)\|^2 \varphi(q_d) \\ & +\rho_1(z_{d1}, z_1, q_d, e)\|\bigtriangledown\varphi(q_d)\|\|\Psi_1(t)\| \\ & +\rho_2(z_{d2}, q_d, e)\|\bigtriangledown\varphi(q_d)\|\|z_d\| \\ & +(\bigtriangledown\varphi(q_d))^T v_r\end{aligned} \tag{38}$$

where the vector $\Psi_1(t) \in \mathbb{R}^3$ is defined as follows

$$\Psi_1(t) = \begin{bmatrix} w, & \tilde{z}^T \end{bmatrix}^T, \tag{39}$$

and the positive function $\rho_1(z_{d1}, z_1, q_d, e)$ and $\rho_2(z_{d1}, z_1, q_d, e)$ are defined in (25). After substituting (24) into (38), $\dot{V}_2(t)$ can be rewritten as follows

$$\dot{V}_2 \leqslant -\|\bigtriangledown\varphi(q_d)\|^2 \varphi(q_d) + \frac{1}{k_3}\left(w^2 + \|\tilde{z}\|^2\right) + \frac{1}{k_4}\|z_d\|^2. \tag{40}$$

Based on (35) and (40), the time derivative of $V(t)$ in (32) can be upper bounded by the following inequality

$$\begin{aligned}\dot{V} &\leqslant -\bar{k}_1 w^2 - \bar{k}_2 \|\tilde{z}\|^2 \\ &\quad - \|\nabla\varphi(q_d)\|^2 \varphi(q_d) + \frac{1}{k_4}\|z_d\|^2\end{aligned} \tag{41}$$

where the positive constant $\bar{k}_1, \bar{k}_2 \in \mathbb{R}$ are defined as follows

$$\bar{k}_1 \triangleq kk_1 - \tfrac{1}{k_3} \qquad \bar{k}_2 \triangleq kk_2 - \tfrac{1}{k_3} \ .$$

Case 1: If $\|\nabla\varphi(q_d)\|^2 \leqslant \varepsilon_z$, from the Property 4 in Definition 1, it is clear that

$$\|q_d(t) - q^*\| \leqslant \varepsilon_r$$

Case 2: If $\|\nabla\varphi(q_d)\|^2 \geqslant \varepsilon_z$, it is clear from (32), (33), (34), and (41) that

$$\dot{V} \leqslant -\epsilon_z V + \epsilon_F \tag{42}$$

where $\epsilon_z \triangleq \min\left\{\frac{1}{k}\bar{k}_1, \frac{1}{k}\bar{k}_2, \varepsilon_z\right\}$, and $\epsilon_F \triangleq \frac{1}{k_4}\|z_d\|^2$ are positive constants. Based on (42), $V(t)$ can be upper bounded as follows

$$V(t) \leqslant V(0)\exp(-\epsilon_z t) + \frac{\epsilon_F}{\epsilon_z}(1 - \exp(-\epsilon_z t)) \tag{43}$$

therefore

$$V(t) \leqslant V(0) + \frac{\epsilon_F}{\epsilon_z}. \tag{44}$$

Based on (32), (34), and (44), it is clear that

$$\varphi(q_d(t)) \leqslant \varphi(q_d(0)) + k\left(V_1(0) + \frac{\epsilon_F}{\epsilon_z}\right). \tag{45}$$

If $q_d(0)$ is not on the boundary of $\mathcal{D}$, $\varphi(q_d(0)) < 1$. Then k can be adjusted to ensure

$$\varphi(q_d(0)) + k\left(V_1(0) + \frac{\epsilon_F}{\epsilon_z}\right) < 1. \tag{46}$$

Based on (45) and (46), $\varphi(q_d(t)) < 1$, hence $q_d(t) \in \mathcal{D}$ from Definition 1. It is clearly from (43) that $\varphi(q_d)$ is ultimately bounded by $\frac{\epsilon_F}{\epsilon_z}$. Therefore, if $\|\nabla\varphi(q_d)\|^2 \geqslant \varepsilon_z$, k_4 can be adjusted to ensure $\frac{\epsilon_F}{\epsilon_z} = \varepsilon$, where ε is defined in Definition 1. Hence by the Property 5 in Definition 1, $\|q_d(t) - q^*\|$ is ultimately bounded by ε_r. □

Theorem 2 *The kinematic control law given in (15)-(19) ensures global uniformly ultimately bounded (GUUB) position and orientation tracking in the sense that*

$$|\tilde{x}(t)|, |\tilde{y}(t)|, \left|\tilde{\theta}(t)\right| \leqslant \varepsilon_2 \exp(-\gamma_0 t) + \varepsilon_3\varepsilon_1 \tag{47}$$

where ε_1 was given in (19), $\varepsilon_2 \triangleq \sqrt{w^2(0) + z_1^2(0) + z_2^2(0)}$, and ε_3 and γ_0 are positive constants.

Proof: Based on (33) and (35), $\dot{V}_1(t)$ of (35) can be upper bounded as follows

$$\dot{V}_1 \leqslant -2\min\left\{\ k_1, \quad k_2\ \right\} V_1. \tag{48}$$

Based on (48), the following inequality can be obtained

$$V_1(t) \leqslant \exp\left(-2\min\left\{\ k_1, \quad k_2\ \right\} t\right) V_1(0). \tag{49}$$

Based on (33), (49) can be rewritten as follows

$$\|\Psi_1(t)\| \leqslant \exp\left(-\min\left\{\ k_1, \quad k_2\ \right\} t\right) \|\Psi_1(0)\| \tag{50}$$

where the vector $\Psi_1(t)$ is defined in (39).

From (33) and (49), it is clear that $w(t), \tilde{z}(t) \in \mathcal{L}_\infty$. Based on (19) and (20), we can conclude that $z_d(t) \in \mathcal{L}_\infty$. From (14) and $\tilde{z}(t), z_d(t) \in \mathcal{L}_\infty$, it is clear that $z(t) \in \mathcal{L}_\infty$. Since $w(t), z(t) \in \mathcal{L}_\infty$, based on the inverse transformation from (9), $e(t) \in \mathcal{L}_\infty$. Based on $q_d(t) \in \mathcal{L}_\infty$ from Theorem 1 and $e(t) \in \mathcal{L}_\infty$, it is clear that $q(t) \in \mathcal{L}_\infty$. From (22)-(25), $q_d(t), z_d(t), z(t), e(t) \in \mathcal{L}_\infty$, and the properties in Definition 1, we can conclude that $v_r(t)$, $\dot{q}_d(t) \in \mathcal{L}_\infty$. Based on (12) and $q(t), z(t), \dot{q}_d(t) \in \mathcal{L}_\infty$, $f(\theta, z_2, \dot{q}_d) \in \mathcal{L}_\infty$. Then $\Omega_1(t) \in \mathcal{L}_\infty$ from (18). Then $u(t), u_a(t), \dot{z}_d(t) \in \mathcal{L}_\infty$ from (15)-(17). Based on the fact that $f(\theta, z_2, \dot{q}_d), z(t), u(t) \in \mathcal{L}_\infty$, then (10) can be used to conclude $\dot{w}(t), \dot{z}(t) \in \mathcal{L}_\infty$. It is clear from $\dot{z}(t), \dot{z}_d(t) \in \mathcal{L}_\infty$ that $\dot{\tilde{z}}\ (t) \in \mathcal{L}_\infty$. Then standard signal chasing arguments can be employed to conclude that all of the remaining signals in the control and the system remain bounded during closed-loop operation.

Based on (19), (20), (39), and (50), the triangle inequality can be applied to (14) to prove that

$$\begin{aligned}\|z\| &\leqslant \|\tilde{z}\| + \|z_d\| \\ &\leqslant \exp\left(-\min\left\{\ k_1, \quad k_2\ \right\} t\right) \|\Psi_1(0)\| \\ &\quad + \alpha_0 \exp(-\alpha_1 t) + \varepsilon_1.\end{aligned} \tag{51}$$

Utilizing (50)-(51), the result given in (47) can be obtained from taking the inverse of the transformation given in (9). □

Remark 2 *Although $q_d(t)$ is a collision-free path, the stability result in Theorem 2 only ensures practical tracking of the path in the sense that the actual WMR trajectory is only guaranteed to remain in a neighborhood of the desired path. From (5) and (47), the following bound can be developed*

$$\|q\| \leq \|q_d\| + \sqrt{3}\varepsilon_2 \exp(-\gamma_0 t) + \sqrt{3}\varepsilon_3\varepsilon_1 \tag{52}$$

where $q_d(t) \in \mathcal{D}$ based on the proof for Theorem 1. To ensure that $q(t) \in \mathcal{D}$, the free configuration space needs to be reduced to incorporate the effects of the second and third terms on the right hand side of (52). To

this end, the size of the obstacles could be increased by $\sqrt{3}(\varepsilon_2 + \varepsilon_3\varepsilon_1)$*, where* $\varepsilon_3\varepsilon_1$ *can be made arbitrarily small by adjusting the control gains. To minimize the effects of* ε_2*, the initial conditions* $w(0)$ *and* $z(0)$ *(and hence,* $\tilde{x}(0), \tilde{y}(0), \tilde{\theta}(0)$*) could be required to be sufficiently small enough to yield a feasible path to the goal.*

5 Online 2D Navigation

In the previous approach, the size of the obstacles is required to be increased due to the fact that the navigation-like function is formulated in terms of the desired trajectory. In the following approach, the navigation function proposed in [22] is formulated based on current position feedback, and hence, $q(t)$ can be proven to be a member of $\mathcal{D}$ without placing restrictions on the initial conditions.

5.1 Trajectory Planning

Let $\varphi(x_c, y_c) \in \mathbb{R}$ denote a 2D position-based navigation function defined in $\mathcal{D}$ that is generated online, where the gradient vector of $\varphi(x_c, y_c)$ is defined as follows

$$\nabla\varphi(x_c, y_c) \triangleq \left[\begin{array}{cc} \frac{\partial\varphi}{\partial x_c} & \frac{\partial\varphi}{\partial y_c} \end{array} \right]^T. \tag{53}$$

Let $\theta_d(x_c, y_c) \in \mathbb{R}$ denote a desired orientation that is defined as a function of the negated gradient of the 2D navigation function as follows

$$\theta_d \triangleq \arctan 2\left(-\frac{\partial\varphi}{\partial y_c}, \quad -\frac{\partial\varphi}{\partial x_c} \right) \tag{54}$$

where $\arctan 2(\cdot) : \mathbb{R}^2 \to \mathbb{R}$ denotes the four quadrant inverse tangent function [26], where $\theta_d(t)$ is confined to the following region

$$-\pi < \theta_d \leqslant \pi.$$

As stated in [21], by defining $\theta_d|_{(x_c^*, y_c^*)} = \arctan 2(0,0) = \theta|_{(x_c^*, y_c^*)}$, then $\theta_d(t)$ remains continuous along any approaching direction to the goal position. See Appendix for an expression for $\dot{\theta}_d(t)$ based on the previous continuous definition for $\theta_d(t)$.

Remark 3 *As discussed in [22], the construction of the function* $\varphi(q(t))$*, coined a navigation function, that satisfies the first three properties in Definition 1 for a general obstacle avoidance problem is nontrivial. Indeed, for a typical obstacle avoidance, it does not seem possible to construct* $\varphi(q(t))$ *such that* $\frac{\partial}{\partial q}\varphi(q(t)) = 0$ *only at* $q(t) = q^*$*. That is, as discussed in [22], the appearance of interior saddle points (i.e., unstable equilibria) seems to be unavoidable; however, these unstable equilibria do not really cause any difficulty in practice. That is,* $\varphi(q(t))$ *can be constructed as shown in [22] such that only a "few" initial conditions will actually get stuck on the unstable equilibria.*

5.2 Control Development

Based on the open-loop system introduced in (1)-(4) and the subsequent stability analysis, the linear velocity control input $v_c(t)$ is designed as follows

$$v_c \triangleq k_v \|\nabla\varphi\| \cos\tilde{\theta} \tag{55}$$

where $k_v \in \mathbb{R}$ denotes a positive, constant control gain, and $\tilde{\theta}(t)$ was introduced in (5). After substituting (55) into (1), the following closed-loop system can be obtained

$$\left[\begin{array}{c} \dot{x}_c \\ \dot{y}_c \end{array} \right] = k_v \left[\begin{array}{c} \cos\theta \\ \sin\theta \end{array} \right] \|\nabla\varphi\| \cos\tilde{\theta}. \tag{56}$$

The open-loop orientation tracking error system can be obtained by taking the time derivative of $\tilde{\theta}(t)$ in (5) as follows

$$\dot{\tilde{\theta}} = \omega_c - \dot{\theta}_d \tag{57}$$

where (1) was utilized. Based on (57), the angular velocity control input $\omega_c(t)$ is designed as follows

$$\omega_c \triangleq -k_\omega\tilde{\theta} + \dot{\theta}_d \tag{58}$$

where $k_\omega \in \mathbb{R}$ denotes a positive, constant control gain, and $\dot{\theta}_d(t)$ denotes the time derivative of the desired orientation. See Appendix for an explicit expression for $\dot{\theta}_d(t)$. After substituting (58) into (57), the closed-loop orientation tracking error system is given by the following linear relationship

$$\dot{\tilde{\theta}} = -k_\omega\tilde{\theta}. \tag{59}$$

Linear analysis techniques can be used to solve (59) as follows

$$\tilde{\theta}(t) = \tilde{\theta}(0)\exp(-k_\omega t). \tag{60}$$

After substituting (60) into (56) the following closed-loop error system can be determined

$$\left[\begin{array}{c} \dot{x}_c \\ \dot{y}_c \end{array} \right] = k_v \left[\begin{array}{c} \cos\theta \\ \sin\theta \end{array} \right] \|\nabla\varphi\| \cos\left(\tilde{\theta}(0)\exp(-k_\omega t)\right). \tag{61}$$

5.3 Stability Analysis

Theorem 3 *The control input designed in (55) and (58) along with the navigation function* $\varphi(x_c(t), y_c(t))$ *ensure asymptotic navigation in the sense that*

$$|x(t) - x^*|, |y(t) - y^*|, \left|\tilde{\theta}(t)\right| \to 0 \text{ as } t \to \infty. \tag{62}$$

Proof: Let $V_3(x_c, y_c) : \mathcal{D} \to \mathbb{R}$ denote the following non-negative function

$$V_3(x_c, y_c) \triangleq \varphi(x_c, y_c). \tag{63}$$

After taking the time derivative of (63) and utilizing (1), (53), and (56), the following expression can be obtained

$$\dot{V}_3 = k_v \left(\nabla\varphi\right)^T \begin{bmatrix} \cos\theta \\ \sin\theta \end{bmatrix} \|\nabla\varphi\| \cos\tilde{\theta}. \quad (64)$$

Based on the development provided in Appendix, the gradient of the navigation function can be expressed as follows

$$\nabla\varphi = -\|\nabla\varphi\| \begin{bmatrix} \cos\theta_d & \sin\theta_d \end{bmatrix}^T. \quad (65)$$

After substituting (65) into (64), the following expression can be obtained

$$\dot{V}_3 = -k_v \|\nabla\varphi\|^2 \left(\cos\theta\cos\theta_d + \sin\theta\sin\theta_d\right)\cos\tilde{\theta}. \quad (66)$$

After utilizing a trigonometric identity, (66) can be rewritten as follows

$$\dot{V}_3 = -g(t) \quad (67)$$

where $g(t) \in \mathbb{R}$ denotes the following positive function

$$g(t) \triangleq k_v \|\nabla\varphi\|^2 \cos^2\tilde{\theta}. \quad (68)$$

Based on (53) and the property of the navigation function (Similar to the Property 1 of Definition 1), it is clear that $\|\nabla\varphi\left(x_c, y_c\right)\| \in \mathcal{L}_\infty$ on $\mathcal{D}$; hence, (55) can be used to conclude that $v_c\left(t\right) \in \mathcal{L}_\infty$ on $\mathcal{D}$. Development is also provided in the Appendix that proves $\dot{\theta}_d\left(t\right) \in \mathcal{L}_\infty$ on $\mathcal{D}$; hence, (58) can be used to show that $\omega_c\left(t\right) \in \mathcal{L}_\infty$ on $\mathcal{D}$. Based on the fact that $v_c\left(t\right) \in \mathcal{L}_\infty$ on $\mathcal{D}$, (1)-(4) can be used to prove that $\dot{x}_c\left(t\right)$, $\dot{y}_c\left(t\right) \in \mathcal{L}_\infty$ on $\mathcal{D}$. After taking the time derivative of (53) the following expression can be obtained

$$\frac{d}{dt}\left(\nabla\varphi\left(x_c, y_c\right)\right) = \begin{bmatrix} \dfrac{\partial^2\varphi}{\partial x_c^2} & \dfrac{\partial^2\varphi}{\partial y_c \partial x_c} \\ \dfrac{\partial^2\varphi}{\partial x_c \partial y_c} & \dfrac{\partial^2\varphi}{\partial y_c^2} \end{bmatrix} \begin{bmatrix} \dot{x}_c \\ \dot{y}_c \end{bmatrix}. \quad (69)$$

Since $\dot{x}_c\left(t\right)$, $\dot{y}_c\left(t\right) \in \mathcal{L}_\infty$ on $\mathcal{D}$, and since each element of the Hessian matrix in (69) is bounded by the property of the navigation function (Similar to the Property 1 of Definition 1), it is clear that $\dot{g}(t) \in \mathcal{L}_\infty$ on $\mathcal{D}$. Based on (63), (67), (68), and the fact that $\dot{g}(t) \in \mathcal{L}_\infty$ on $\mathcal{D}$, then Lemma A.6 of [6] can be invoked to prove that

$$\|\nabla\varphi\left(x_c, y_c\right)\|^2 \cos^2\tilde{\theta} \to 0 \quad (70)$$

in the region $\mathcal{D}$. Based on the fact that $\cos^2\tilde{\theta}(t) \to 1$ from (60), then (70) can be used to prove that $\|\nabla\varphi\left(x_c, y_c\right)\| \to 0$. Therefore the result in (62) can be obtained based on the analysis in Remark 3. □

Remark 4 *The control development in this section is based on a 2D position navigation function. To achieve the objective, a desired orientation $\theta_d\left(t\right)$ was defined as a function of the negated gradient of the 2D navigation function. The previous development can be used to prove the result in (62). If a navigation function $\varphi\left(x_c, y_c\right)$ can be found such that $\theta_d|_{(x_c^*, y_c^*)} = \theta^*$, then asymptotic navigation can be achieved by the controller in (55) and (58); otherwise, a standard regulation controller (e.g., see [8] for several candidates) could be implemented to regulate the orientation of the WMR from $\theta_d|_{(x_c^*, y_c^*)} \to \theta^*$. Alternatively, a dipolar potential field approach [23], [24] or a virtual obstacle [9] could be utilized to align the gradient field of the navigation function to the goal orientation of the WMR.*

6 Simulation Results

To illustrate the performance of the controller given in (55) and (58), a numerical simulation was performed to navigate the WMR from $q\left(x_c\left(0\right), y_c\left(0\right), \theta\left(0\right)\right)$ to $q^*\left(x_c^*, y_c^*, \theta^*\right)$. Since the properties of a navigation function are invariant under a diffeomorphism, a diffeomorphism is developed to map the WMR free configuration space to a model space [17]. Specifically, a positive function $\varphi\left(x_c, y_c\right)$ was chosen as follows

$$\varphi\left(x_c, y_c\right) = \frac{\left(x_c - x_c^*\right)^2 + \left(y_c - y_c^*\right)^2}{\left(\left(\left(x_c - x_c^*\right)^2 + \left(y_c - y_c^*\right)^2\right)^\kappa + \beta_0\beta_1\right)^{1/\kappa}}. \quad (71)$$

where κ is positive integer parameter, and the boundary function $\beta_0\left(x_c, y_c\right) \in \mathbb{R}$ and the obstacle function $\beta_1\left(x_c, y_c\right) \in \mathbb{R}$ are defined as follows

$$\begin{aligned} \beta_0 &\triangleq r_0^2 - \left(x_c - x_{r_0}\right)^2 - \left(y_c - y_{r_0}\right)^2 \\ \beta_1 &\triangleq \left(x_c - x_{r_1}\right)^2 + \left(y_c - y_{r_1}\right)^2 - r_1^2. \end{aligned} \quad (72)$$

In (72), $\left(x_{r_0}, y_{r_0}\right)$ and $\left(x_{r_1}, y_{r_1}\right)$ are the centers of the boundary and the obstacle respectively, r_0, $r_1 \in \mathbb{R}$ are the radii of the boundary and the obstacle respectively. From (71) and (72), it is clear that the model space is a unit circle that excludes a circle described by the obstacle function $\beta_1\left(x_c, y_c\right)$. If more obstacles are present, the corresponding obstacle functions can be easily incorporated into the navigation function [17]. In [17], Koditschek proved that $\varphi\left(x_c, y_c\right)$ in (71) is the navigation function for $\left(x_c\left(t\right), y_c\left(t\right)\right)$, provided that κ is big enough. For the simulation, the model space configuration is selected as follows

$$\begin{aligned} x_{r_0} = 0 \quad y_{r_0} = 0 \quad r_0 = 1 \\ x_{r_1} = 0 \quad y_{r_1} = 0.1 \quad r_1 = 0.15 \end{aligned}$$

where the initial and goal configuration were selected as

$$q\left(0\right) = \begin{bmatrix} 0.1 & 0.6 & 51.6 \end{bmatrix}^T$$

$$q^* = \begin{bmatrix} -0.2 & -0.4 & -40.1 \end{bmatrix}^T.$$

The control inputs defined in (55) and (58) were utilized to drive the WMR to the goal point along the negated gradient angle. The control gains k_v and k_ω were adjusted to the following values to yield the best performance

$$k_v = 0.3 \quad k_\omega = 17. \tag{73}$$

Once the WMR reached the goal position, the regulation controller in [8] was implemented to regulate the WMR from $\theta_d|_{(x_c^*, y_c^*)} \to \theta^*$. The actual trajectory of WMR is shown in Figure 1. The outer circle in Figure 1 depicts the outer boundary of the obstacle free space and the inner circle represents the boundary around an obstacle. The resulting position and orientation errors for the WMR are depicted in Figure 2, where the rotational error shown in Figure 2 is the error between the actual orientation and goal orientation. The control input velocities $v_c(t)$ and $\omega_c(t)$ defined in (55) and (58), respectively, are depicted in Figure 3. Note that the angular velocity input was artificially saturated between $\pm 90[\deg \cdot s^{-1}]$.

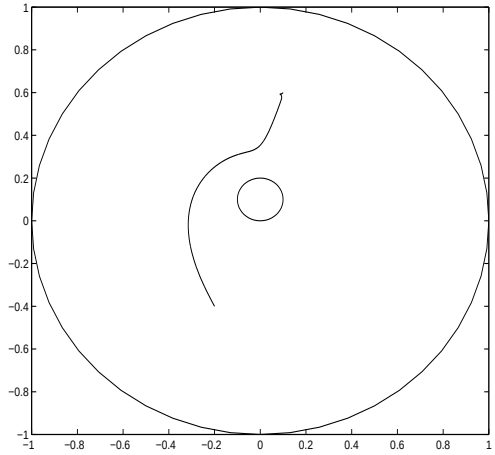

Figure 1: Actual trajectory of the WMR.

7 Conclusions

Two approaches are developed to incorporate navigation function approach into different controllers for task execution by a WMR in the presence of known obstacles. The first approach utilizes a navigation-like function that is based on 3D position and orientation information. The navigation-like function yields a path from an initial configuration inside the free configuration space to a goal configuration. A differentiable, oscillator-based controller is then used to enable the mobile robot to follow the path and stop at the goal position. Using this approach, a WMR was proven to yield uniformly ultimately bounded path following and

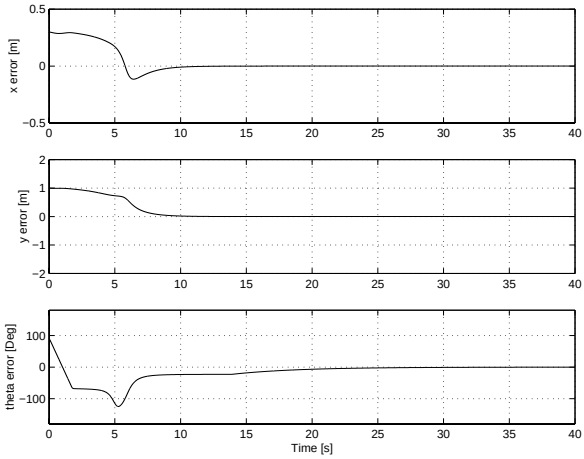

Figure 2: Position and orientation errors.

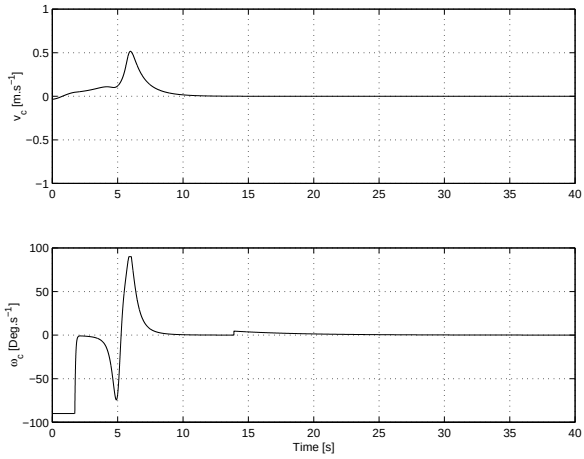

Figure 3: Linear and angular velocity inputs.

regulation to the goal point with an arbitrarily defined goal orientation (i.e., the WMR is not required to spin in place at the goal position to achieve a desired orientation). A second approach is developed that uses a navigation function that is constructed using 2D position information. A differentiable controller is proposed based on this navigation function. The advantage of this approach is that it yields asymptotic position convergence; however, the WMR cannot stop at an arbitrary orientation without additional development. Simulation results are provided to illustrate the performance of the second approach.

References

[1] A. Bemporad, A. De Luca, and G. Oriolo, "Local Incremental Planning for a Car-Like Robot Navigating Among Obstacles," *Proceedings of the IEEE International Conference on Robotics and Automation*, Minneapolis, Minnesota, April 1996, pp. 1205-1211.

[2] J. Barraquand and J. C. Latombe, "A Monte-Carlo Algorithm for Path Planning with Many Degrees of Freedom," *Proceedings of the IEEE International Conference on Robotics and Automation*, Cincinnati, Ohio, May 1990, pp. 584-589.

[3] J. Barraquand, B. Langlois, and J. C. Latombe, "Numerical Potential Fields Techniques for Robot Path Planning," *IEEE Transactions on Systems, Man, and Cybernetics*, Vol. 22, pp. 224-241, (1992).

[4] I. Cervantes, R. Kelly, J. Alvarez-Ramirez, and J. Moreno, "A Robust Velocity Field Control," *IEEE Transactions on Control Systems Technology*, Vol. 10, No. 6, pp. 888-894, (2002).

[5] C. I. Connolly, J. B. Burns, and R. Weiss, "Path Planning Using Laplace's Equation," *Proceedings of the IEEE International Conference on Robotics and Automation*, Cincinnati, Ohio, May 1990, pp. 2102-2106.

[6] M.S. de Queiroz, D.M. Dawson, S.P. Nagarkatti, and F. Zhang, *Lyapunov-Based Control of Mechanical Systems*, Birkhäuser, 1999.

[7] W. E. Dixon, D. M. Dawson, E. Zergeroglu, and F. Zhang, "Robust Tracking and Regulation Control for Mobile Robots," *International Journal of Robust and Nonlinear Control*, Vol. 10, pp. 199-216, (2000).

[8] W. E. Dixon, D. M. Dawson, E. Zergeroglu, and A. Behal, *Nonlinear Control of Wheeled Mobile Robots*, Springer-Verlag London Limited, 2001.

[9] S. S. Ge and Y. J. Cui, "New Potential Functions for Mobile Robot Path Planning," *IEEE Transactions on Robotics and Automation*, Vol. 16, No. 5, pp. 615-620, (2000).

[10] J. Guldner and V. I. Utkin, "Sliding Mode Control for Gradient Tracking and Robot Navigation Using Artificial Potential Fields," *IEEE Transactions on Robotics and Automation*, Vol. 11, No. 2, pp. 247-254, (1995).

[11] J. Guldner, V. I. Utkin, H. Hashimoto, and F. Harashima, "Tracking Gradients of Artificial Potential Field with Non-Holonomic Mobile Robots," *Proc. of the American Control Conference*, Seattle, Washington, June 1995, pp. 2803-2804.

[12] H. K. Khalil, *Nonlinear Systems*, third edition, Prentice Hall, 2002.

[13] O. Khatib, *Commande dynamique dans l'espace opérational des robots manipulateurs en présence d'obstacles*, Ph.D. Dissertation, École Nationale Supéieure de l'Aeéronatique et de l'Espace (ENSAE), France, 1980.

[14] O. Khatib, "Real-Time Obstacle Avoidance for Manipulators and Mobile Robots," *International Journal of Robotics Research*, Vol. 5, No. 1, pp. 90-99, (1986).

[15] K. J. Kyriakopoulos, H. G. Tanner, and N. J. Krikelis, "Navigation of Nonholonomic Vehicles in Complex Environments with Potential Fields and Tracking," *Int. J. Intell. Contr. Syst.*, Vol. 1, No. 4, pp. 487-495, (1996).

[16] D. E. Koditschek, "Exact Robot Navigation by Means of Potential Functions: Some Topological Considerations," *Proc. of the IEEE International Conference on Robotics and Automation*, Raleigh, North Carolina, May 1987, pp. 1-6.

[17] D. E. Koditschek and E. Rimon, "Robot Navigation Functions on Manifolds with Boundary," *Adv. Appl. Math.*, Vol. 11, pp. 412-442, (1990).

[18] J. P. Laumond, P. E. Jacobs, M. Taix, and R. M. Murray, "A Motion Planner for Nonholonomic Mobile Robots," *IEEE Transactions on Robotics and Automation*, Vol. 10, No. 5, pp. 577-593, (1994).

[19] J. C. Latombe, *Robot Motion Planning*, Kluwer Academic Publishers: Boston, Massachusetts, 1991.

[20] P. Li and R. Horowitz, "Passive Velocity Field Control of Mechanical Manipulators," *IEEE Transactions on Robotics and Automation*, Vol. 15, No. 4, pp. 751-763, (2003).

[21] A. De Luca and G. Oriolo, "Local Incremental Planning for Nonholonomic Mobile Robots," *Proc. of the IEEE International Conference on Robotics and Automation*, San Diego, California, May 1994, pp. 104-110.

[22] E. Rimon and D. E. Koditschek, "Exact Robot Navigation Using Artificial Potential Function," *IEEE Transactions on Robotics and Automation*, Vol. 8, No. 5, pp. 501-518, (1992).

[23] H. G. Tanner and K. J. Kyriakopoulos, "Nonholonomic Motion Planning for Mobile Manipulators," *Proc. of the IEEE International Conference on Robotics and*

Automation, San Francisco, California, April 2000, pp. 1233-1238.

[24] H. G. Tanner, S. G. Loizou, and K. J. Kyriakopoulos, "Nonholonomic Navigation and Control of Cooperating Mobile Manipulators," *IEEE Transactions on Robotics and Automation*, Vol. 19, No. 1, pp. 53-64, (2003).

[25] R. Volpe and P. Khosla, "Artificial Potential with Elliptical Isopotential Contours for Obstacle Avoidance," *Proc. of the IEEE Conference on Decision and Control*, Los Angeles, California, December 1987, pp. 180-185.

[26] E. W. Weisstein, *CRC Concise Encyclopedia of Mathematics*, Second Edition, CRC Press, 2002.

Appendix

Based on the definition of $\theta_d(t)$ in (54), $\theta_d(t)$ can be expressed in terms of the natural logarithm as follows [26]

$$\theta_d = -i \ln \left(\frac{-\frac{\partial \varphi}{\partial x_c} - i\frac{\partial \varphi}{\partial y_c}}{\sqrt{\left(\frac{\partial \varphi}{\partial x_c}\right)^2 + \left(\frac{\partial \varphi}{\partial y_c}\right)^2}} \right) \tag{74}$$

where $i{=}\sqrt{-1}$. After exploiting the following identities [26]

$$\begin{aligned} \cos(\theta_d) &= \frac{1}{2}\left(e^{i\theta_d} + e^{-i\theta_d}\right) \\ \sin(\theta_d) &= \frac{1}{2i}\left(e^{i\theta_d} - e^{-i\theta_d}\right) \end{aligned}$$

and then utilizing (74) the following expressions can be obtained

$$\cos(\theta_d) = -\frac{\frac{\partial \varphi}{\partial x_c}}{\sqrt{\left(\frac{\partial \varphi}{\partial x_c}\right)^2 + \left(\frac{\partial \varphi}{\partial y_c}\right)^2}} \tag{75}$$

$$\sin(\theta_d) = -\frac{\frac{\partial \varphi}{\partial y_c}}{\sqrt{\left(\frac{\partial \varphi}{\partial x_c}\right)^2 + \left(\frac{\partial \varphi}{\partial y_c}\right)^2}}. \tag{76}$$

After utilizing (75) and (76), the following expression can be obtained

$$\begin{bmatrix} \frac{\partial \varphi}{\partial x_c} \\ \frac{\partial \varphi}{\partial y_c} \end{bmatrix} = -\sqrt{\left(\frac{\partial \varphi}{\partial x_c}\right)^2 + \left(\frac{\partial \varphi}{\partial y_c}\right)^2} \begin{bmatrix} \cos(\theta_d) \\ \sin(\theta_d) \end{bmatrix}. \tag{77}$$

Based on the expression in (74), the time derivative of $\theta_d(t)$ can be written as follows

$$\dot{\theta}_d = \begin{bmatrix} \frac{\partial \theta_d}{\partial x_c} & \frac{\partial \theta_d}{\partial y_c} \end{bmatrix} \begin{bmatrix} \dot{x}_c \\ \dot{y}_c \end{bmatrix} \tag{78}$$

where

$$\frac{\partial \theta_d}{\partial x_c} = \begin{bmatrix} \frac{-\frac{\partial \varphi}{\partial y_c}}{\left(\frac{\partial \varphi}{\partial x_c}\right)^2 + \left(\frac{\partial \varphi}{\partial y_c}\right)^2} & \frac{\frac{\partial \varphi}{\partial x_c}}{\left(\frac{\partial \varphi}{\partial x_c}\right)^2 + \left(\frac{\partial \varphi}{\partial y_c}\right)^2} \end{bmatrix} \cdot \begin{bmatrix} \frac{\partial^2 \varphi}{\partial x_c^2} & \frac{\partial^2 \varphi}{\partial x_c \partial y_c} \end{bmatrix}^T \tag{79}$$

$$\frac{\partial \theta_d}{\partial y_c} = \begin{bmatrix} \frac{-\frac{\partial \varphi}{\partial y_c}}{\left(\frac{\partial \varphi}{\partial x_c}\right)^2 + \left(\frac{\partial \varphi}{\partial y_c}\right)^2} & \frac{\frac{\partial \varphi}{\partial x_c}}{\left(\frac{\partial \varphi}{\partial x_c}\right)^2 + \left(\frac{\partial \varphi}{\partial y_c}\right)^2} \end{bmatrix} \cdot \begin{bmatrix} \frac{\partial^2 \varphi}{\partial y_c \partial x_c} & \frac{\partial^2 \varphi}{\partial y_c^2} \end{bmatrix}^T. \tag{80}$$

After substituting (1), (79), and (80) into (78), the following expression can be obtained

$$\dot{\theta}_d = \begin{bmatrix} \frac{-\frac{\partial \varphi}{\partial y_c}}{\left(\frac{\partial \varphi}{\partial x_c}\right)^2 + \left(\frac{\partial \varphi}{\partial y_c}\right)^2} & \frac{\frac{\partial \varphi}{\partial x_c}}{\left(\frac{\partial \varphi}{\partial x_c}\right)^2 + \left(\frac{\partial \varphi}{\partial y_c}\right)^2} \end{bmatrix} \cdot \begin{bmatrix} \frac{\partial^2 \varphi}{\partial x_c^2} & \frac{\partial^2 \varphi}{\partial y_c \partial x_c} \\ \frac{\partial^2 \varphi}{\partial x_c \partial y_c} & \frac{\partial^2 \varphi}{\partial y_c^2} \end{bmatrix} \begin{bmatrix} \cos\theta \\ \sin\theta \end{bmatrix} v_c. \tag{81}$$

After substituting (55) and (77) into (81), the following expression can be obtained

$$\dot{\theta}_d = k_v \cos\left(\tilde{\theta}\right) \begin{bmatrix} \sin(\theta_d) & -\cos(\theta_d) \end{bmatrix} \cdot \begin{bmatrix} \frac{\partial^2 \varphi}{\partial x_c^2} & \frac{\partial^2 \varphi}{\partial y_c \partial x_c} \\ \frac{\partial^2 \varphi}{\partial x_c \partial y_c} & \frac{\partial^2 \varphi}{\partial y_c^2} \end{bmatrix} \begin{bmatrix} \cos\theta \\ \sin\theta \end{bmatrix}. \tag{82}$$

By part 1 of Definition 1, each element of the Hessian matrix is bounded; hence, from (82), it is straightforward that $\dot{\theta}_d(t) \in \mathcal{L}_\infty$.